

Critical slowing down of fermions near a magnetic quantum phase transition

Chia-Jung Yang,¹ Kristin Kliemt,² Cornelius Krellner,² Johann Kroha,³ Manfred Fiebig,¹ and Shovon Pal^{1,4}

¹*Department of Materials, ETH Zurich, 8093 Zurich, Switzerland*

²*Physikalisches Institut, Goethe-Universität Frankfurt, 60438 Frankfurt, Germany*

³*Physikalisches Institut and Bethe Center for Theoretical Physics, Universität Bonn, 53115 Bonn, Germany*

⁴*School of Physical Sciences, National Institute of Science Education and Research, HBNI, Jatni, 752 050 Odisha, India*

(Dated: August 12, 2022)

A universal phenomenon in phase transitions is critical slowing down (CSD) — systems, after an initial perturbation, take an exceptionally long time to return to equilibrium. It is universally observed in the dynamics of bosonic excitations, like order-parameter collective modes, but it is not generally expected to occur for fermionic excitations because of the half-integer nature of the fermionic spin. Direct observation of CSD in fermionic excitations or quasiparticles would therefore be of fundamental significance. Here, we observe fermionic CSD in the heavy-fermion (HF) compound YbRh_2Si_2 by terahertz time-domain spectroscopy. HFs are compound objects with a strongly enhanced effective mass, composed of itinerant and localized electronic states. We see that near the quantum phase transition in YbRh_2Si_2 the build-up of spectral weight of the HFs towards the Kondo temperature $T_K \approx 25$ K is followed by a logarithmic rise of the quasiparticle excitation rate on the heavy-Fermi-liquid side of the quantum phase transition below 10 K. A critical two-band HF liquid theory shows that this is indicative of fermionic CSD. This CSD is a clear indication that the HF quasiparticles experience a breakdown near the quantum phase transition, and the critical exponent of this breakdown introduces a classification of fermionic quantum phase transitions analogous to thermodynamic phase transitions — solution to a long-standing problem.

At a continuous phase transition, the ordered and the disordered phases become equal in energy. As a consequence, the fluctuations between these two states become infinitely slow. This so-called critical slowing down (CSD) is universally observed in the dynamics of classical fields which are bosonic in nature and vanish at the phase transition, like the magnetization, associated with bosonic magnons, in the case of ferromagnetic order[1]. By contrast, CSD of fermionic excitations or quasiparticles is generally not expected to occur since fermions as elementary particles are thought to be indestructible. However, certain quantum materials known as heavy-fermion (HF) compounds host *composite* fermionic quasiparticles. These are quantum superpositions of itinerant and localized, i.e., heavy, electron states generated by the Kondo effect[2, 3], with a low binding energy parameterized by the Kondo energy scale, the lattice Kondo temperature T_K . At a magnetic quantum phase transition (QPT) in such materials (see Fig. 1a), these brittle, heavy quasiparticles are assumed to disintegrate due to critical fluctuations[4–6] despite their fermionic nature, and fermionic CSD would be a unique signature of this destruction.

Using time-resolved terahertz (THz) spectroscopy, we directly observe such fermionic CSD as a suppression of the heavy-particle hybridization gap and flattening of the associated band. This “softening” expands the region in momentum space where resonant THz absorption is allowed. We observe this as an *increase* instead of a Kondo-weight-loss-generated decrease of the Kondo-related THz signal towards the quantum critical point (QCP) before the heavy quasiparticle band vanishes altogether below a breakdown temperature T_{qp}^* [7]. Moreover, we identify a critical exponent in this behaviour and thus set the stage for the classification of fermionic quantum criticality in analogy to the criticality of thermodynamic phase transitions.

Signatures of Kondo quasiparticle destruction were suspected from the dynamical scaling of the magnetic susceptibility[8],

specific heat measurements[9], Hall effect measurements of the carrier density[10], and optical conductivity measurements[11]. The conjectures entering the interpretation of these measurements have been challenged, however[12, 13]. Time-resolved THz spectroscopy is a unique tool to probe the heavy quasiparticle dynamics and to resolve these questions. Specifically, HF materials respond to an incident ultrashort THz pulse by the emission of a time-delayed reflex[14]. This “echo” is a response from the reconstructing Kondo ground state after its destruction by the incident pulse. Hence, time acts as a filter separating the Kondo-sensitive delayed pulse from the Kondo-insensitive main pulse so that the former is a *background-free response of the HF state*. Specifically, the amplitude and the delay time of the echo pulse are proportional to the HF spectral weight and the Kondo coherence time $\tau_K = 2\pi\hbar/k_B T_K$, respectively (with \hbar the Planck and k_B the Boltzmann constant). As a method, this technique was introduced through experiments on $\text{CeCu}_{6-x}\text{Au}_x$ [14–16].

In YbRh_2Si_2 we now apply this new method to directly measure the fermionic CSD. YbRh_2Si_2 is a prototypical HF compound. In zero magnetic field it is antiferromagnetic below the Néel temperature $T_N = 72$ mK. It undergoes a QPT to a Kondo HF liquid at a critical magnetic field of $B_{\perp} \approx 66$ mT perpendicular to the c axis[17, 18] (see Fig. 1a)) induced by the Ruderman-Kittel-Kasuya-Yosida (RKKY) magnetic interaction between the Yb moments[19–22]. Alternatively, a 6% substitution of Rh by Ir creates a QCP at zero field[23, 24]. YbRh_2Si_2 has a Kondo temperature of $T_K \approx 25$ K, high enough to enable a wide quantum-critical region and to permit us to search for signs of CSD in the range $T_{\text{qp}}^* < T < T_K$, in contrast to the case of $\text{CeCu}_{6-x}\text{Au}_x$. In our temperature-dependent, time-resolved THz reflection spectroscopy measurements we crossed the QCP by varying the magnetic field or the Ir concentration. The 1.5-cycle THz pulses of ~ 2 ps duration were incident onto the c -cut $\text{Yb}(\text{Rh}_{1-x}\text{Ir}_x)_2\text{Si}_2$ samples ($x = 0, 0.06$). The echo pulses were

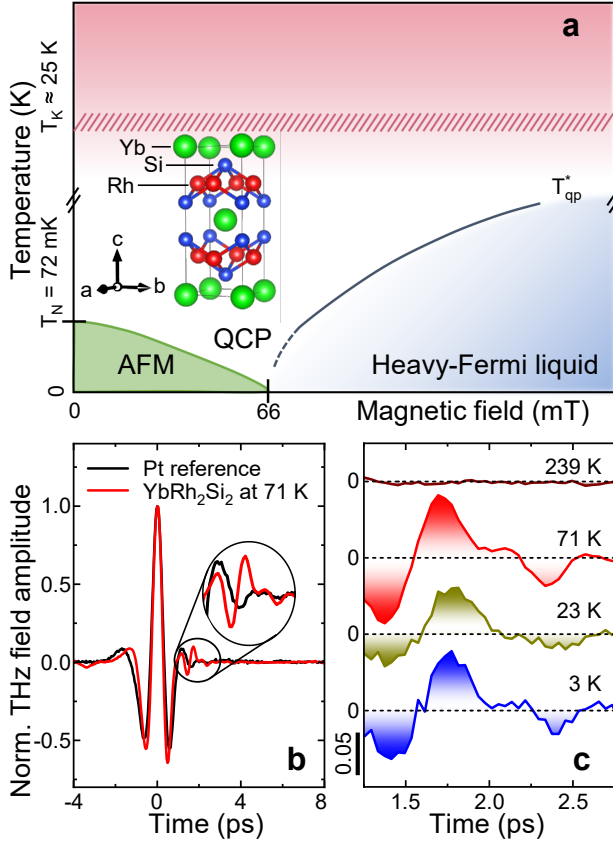


Figure 1. **Exploring fermionic quantum criticality by time-resolved THz reflectivity.** **a**, Schematic phase diagram of YbRh_2Si_2 with characteristic energy scales. **b**, Reflected THz signal from the YbRh_2Si_2 sample (red) and from a Pt mirror reference (black). The time traces are normalized by the maximum field amplitude at $t = 0$ ps. The delayed, purely Kondo-related “echo” pulse is visible in the interval between 1.3 and 2.6 ps, where it distinctly differs from the Pt reference signal. **c**, Signal of the delayed pulse in YbRh_2Si_2 at $B_\perp = 0$ for various temperatures.

analysed as described elsewhere[14]. With $T_K = 25$ K we obtain a delay time $\tau_K \approx 1.9$ ps for these in agreement with the data in Figs. 1b and 1c. We therefore chose the time window for the analysis from 1.3 to 2.6 ps.

Fig. 2 shows the time-integrated intensity of the THz echo pulse for $\text{Yb}(\text{Rh}_{1-x}\text{Ir}_x)_2\text{Si}_2$ for $x = 0$ and $B_\perp = 214$ mT and for $x = 0.06$ and $B_\perp = 0$. All plots exhibit a similar maximum value of the spectral Kondo weight near 25 K in good agreement with T_K . Aside from a shift towards higher temperature right at the QCP, the maximum shows no systematic field dependence. Below the peak temperature, the signal initially decreases with temperature for all magnetic fields. This can be attributed to the reduced thermal broadening of THz-induced interband transitions and is reproduced by the theory introduced below.

On the antiferromagnetic side of the QCP (Figs. 2a and 2b), the signal continues to decrease but remains finite down to the lowest experimentally achieved temperature of 2 K. We note that this temperature and field range ($2.0 \text{ K} \leq T \leq 20 \text{ K}$, $B_\perp \lesssim 66 \text{ mT}$) is within the white area of the phase diagram in Fig. 1a, the so-called quantum-critical fan[9, 24], where ther-

modynamic and transport properties are dominated by quantum-critical fluctuations[11, 17, 18]. However, our THz time-delay spectroscopy is not directly sensitive to these fluctuations, but exclusively to the HF quasiparticle spectral weight[14, 15]. Therefore, the behavior in Figs. 2a and 2b indicates that the Kondo effect remains partially intact in this temperature range. This is reasonable since we are still a factor of ~ 25 above T_N so that the heavy quasiparticles are not entirely destroyed by the impending antiferromagnetic order.

At quantum criticality (Figs. 2d and 2h), the temperature dependence changes drastically. The initial signal decrease with temperature is now followed by a logarithmic *increase* of the THz echo signal that persists down to the lowest observed temperature. Note qualitative similarity between the field-tuned (Fig. 2d) and chemically tuned (Fig. 2h) quantum critical systems, however with different logarithmic slopes. On the HF liquid side of the QCP the signal increase towards the lowest temperatures is still present and gradually fades away with distance from the QCP (Figs. 2e-g). Its onset may also be conjectured at 50 mT on the antiferromagnetic side. (Fig. 2c).

To understand the striking logarithmic increase towards low temperature, we analyze the THz echo signal theoretically. In a HF system, the strongly correlated, flat band produced by the Kondo effect hybridizes with the light conduction band to generate a structure with a lower ($n = 1$) and an upper ($n = 2$) band with avoided crossing[15, 25, 26], as shown in Figs. 3a to 3c. While low-temperature thermodynamic and transport experiments probe the lower, occupied band only, resonant THz spectroscopy involves transitions between both bands, which calls for a two-band theory. Our according, critical HF liquid theory shows (see Methods) that the $n = 1, 2$ bands with dispersions $\epsilon_{n\vec{p}}$ (where \vec{p} is the crystal-electron momentum) have distinct momentum- and temperature-dependent spectral weights $z_{n\vec{p}}$. These cross over from $z_{n\vec{p}} \approx 1$ in the strongly dispersive region to $z_{n\vec{p}} = az_0 \ll 1$ in the flat region of these bands, see Figs. 3d to 3f and insets. Here, $a \ll 1$ is the spectral weight of the local, single-ion Kondo resonance, which builds up logarithmically from above T_K and then saturates towards a constant value for $T < T_K$. Further, $z_0 = (T/T_0)^\alpha$ is a suppression factor with a critical exponent α . It describes the destruction of quasiparticle spectral weight as the QCP is approached by lowering the temperature T below the onset temperature for quantum criticality, T_0 . For the latter, experiments revealed $T_0 \approx T_K$ in YbRh_2Si_2 [27].

As mentioned, the THz echo pulse at $\tau_K = 2\pi\hbar/k_B T_K$ is solely sensitive to the breakup-and-recovery dynamics of the HFs and not to other THz absorption channels[14–16]. Therefore, its intensity exclusively depends on the quasiparticle weight and the phase space available for THz-induced excitations. Specifically, the echo-pulse intensity is proportional to the probability

$$P(T) = A \int d^3p z_{1\vec{p}} z_{2\vec{p}} f(\epsilon_{1\vec{p}}) [1 - f(\epsilon_{2\vec{p}})] W(\Delta\epsilon_{\vec{p}}) \quad (1)$$

for the resonant excitation of electrons from the lower to the upper band at an energy difference $\Delta\epsilon_{\vec{p}} = \epsilon_{2\vec{p}} - \epsilon_{1\vec{p}}$. Here, $f(\epsilon_{n\vec{p}})$ is the Fermi-Dirac distribution function. In Eq. (1), it describes the probability that the $n = 1$ band is occupied and the $n = 2$

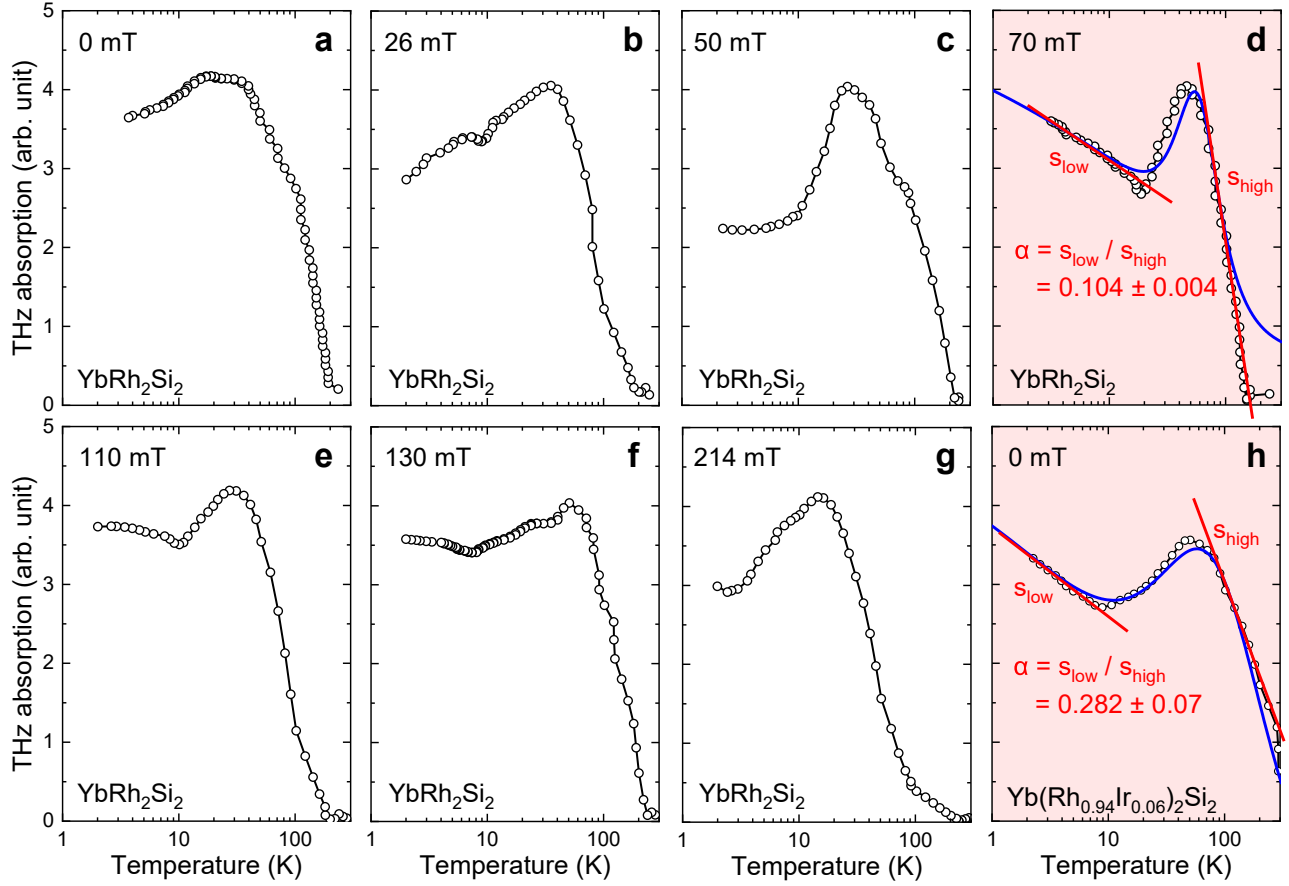


Figure 2. **Temperature dependence of the resonant THz absorption across the QCP in YbRh₂Si₂.** **a–g**, Evolution of the THz absorption by resonant Kondo quasiparticle excitations at various external magnetic fields B_{\perp} as a function of temperature. The weights are derived from the integrated intensity of the echo pulses emitted in the time window of 1.3 – 2.6 ps time window (see Figs. 1b, c). **h**, Temperature dependence of the resonant THz absorption in quantum critical Yb(Rh_{0.94}Ir_{0.06})₂Si₂. Fits of Eq. 1 are plotted as blue lines in **d** and **h**.

band is empty before the THz absorption process. $W(\hbar\omega)$ is the spectrum of the incident THz pulse, which is a Gaussian distribution of width Γ centered around the central frequency Ω_{THz} . With $\Delta\varepsilon_{\vec{p}} \approx \hbar\Omega_{\text{THz}}$, the THz-induced interband transition becomes resonantly allowed. The integral runs over all electron momenta, and the factor A is a temperature-independent constant, proportional to the intensity of the incident THz pulse and to the modulus square of the electric-dipole transition-matrix element between the two bands.

When the probability for HF formation, $az_0 \propto (T/T_K)^\alpha$, tends to zero at the QCP, the heavy bands flatten according to the two-band HF liquid theory. Also, the hybridization gap vanishes, and with that the quasiparticle energy in the heavy regions of both bands ($n = 1, 2$) approaches the Fermi energy E_F , see Figs. 3d to 3f. This means that the oscillation frequency of fermionic quasiparticles, $\omega_{n\vec{p}} = (\varepsilon_{n\vec{p}} - E_F)/\hbar$, vanishes, which is indicative of a fermionic CSD. In turn, it implies an expansion of the region in the momentum space where resonant THz transitions are allowed, seen as broadening of the shaded areas in Figs. 3a to 3c. The interplay of these two counteracting effects, quasiparticle destruction and phase-space expansion, leads to a non-monotonic temperature dependence of the THz absorption

strength $P(T)$. An expansion of Eq. (1) for small $z_0(T)$ predicts a logarithmic increase of $P(T) \propto \ln[1/z_0(T)]$ towards low temperatures down to the region of T_{qp}^* . The full numerical evaluation of Eq. 1 leads to the behavior shown in Fig. 3g. It reproduces the Kondo maximum near $T_K \approx 25$ K and at quantum criticality indeed to a logarithmic increase across an intermediate temperature window $T_{\text{qp}}^* < T < T_K$ according to

$$P(T) = \alpha A \ln(T_K/T) \quad , \quad (2)$$

observing this behavior in Figs. 2d and 2h is thus a unique experimental signature of fermionic quasiparticle CSD in the Yb(Rh_{1-x}Ir_x)₂Si₂ system.

Upon further decreasing the temperature to $T < T_{\text{qp}}^*$, $P(T)$ approaches zero as the HF weight disappears altogether, see inset of Fig. 3g. The low-temperature scale T_{qp}^* is thus defined as the position of the signal maximum between the logarithmic increase and its ultimate collapse towards $T \rightarrow 0$. As seen in Fig. 3g (inset), T_{qp}^* depends on the critical exponent α and is several orders of magnitude lower than the Kondo scale $\sim T_K$, possibly undetectably small. A low-temperature scale T^* has also been observed as a maximum in the magnetic susceptibility[24] whose microscopic origin has, however, remained unclear. Since

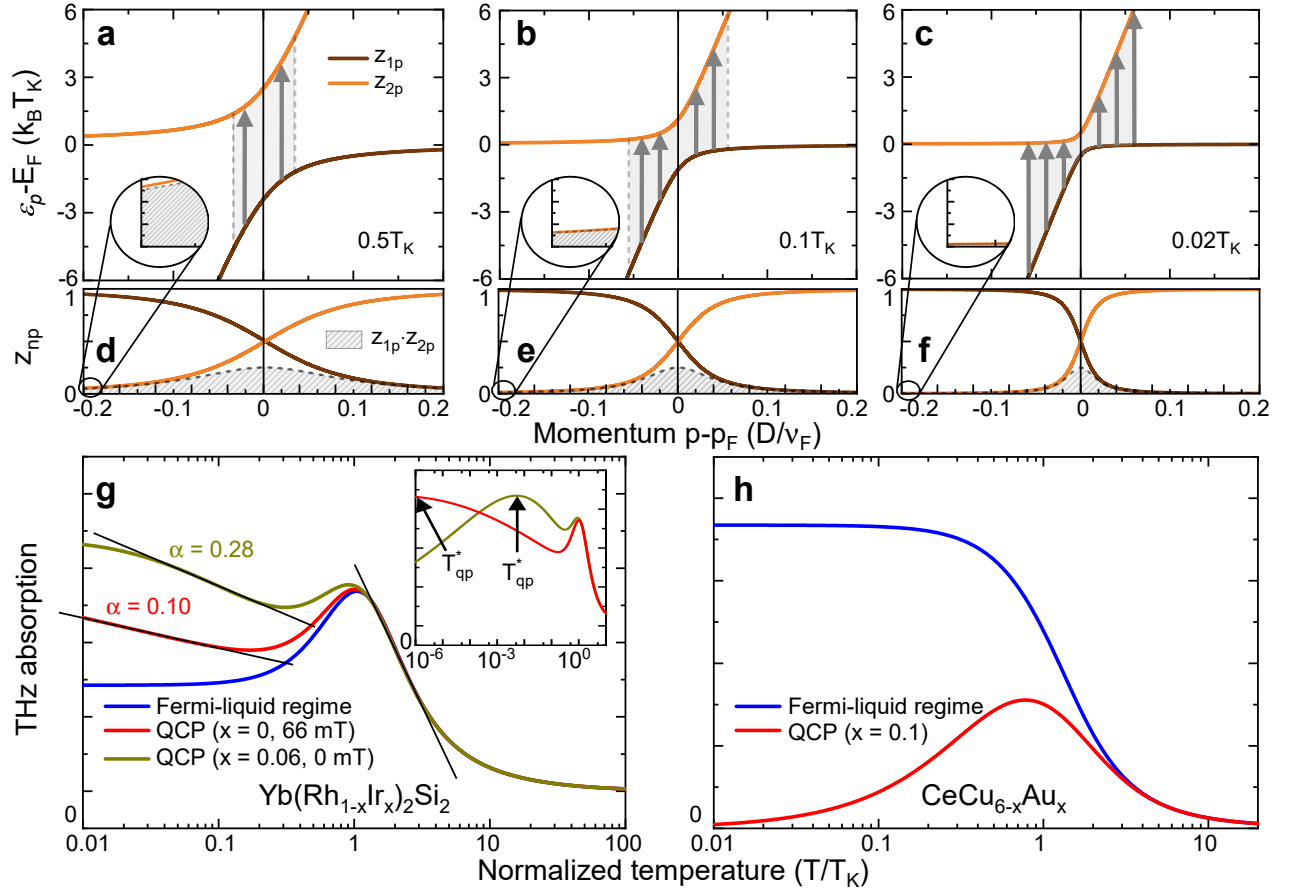


Figure 3. **Band structure and Kondo weight calculations towards the QCP.** **a–c**, Band structure of the conduction band (steep slope) and the Kondo state (flat band) resulting in a hybridized lower (brown) and upper (orange) branch. **d–f**, Momentum- and temperature-dependent quasiparticle weights $z_{1\bar{p}}$, $z_{2\bar{p}}$ in the lower (brown) and upper (orange) bands as well as the product $z_{1\bar{p}} \cdot z_{2\bar{p}}$, all calculated from the two-band critical Fermi liquid theory. **g, h**, Resonant THz absorption strength at (red and dark yellow) and away from (blue) the QCP as calculated for the system parameters of $\text{Yb}(\text{Rh}_{1-x}\text{Ir}_x)_2\text{Si}_2$, ($x = 0, 0.06$) and $\text{CeCu}_{6-x}\text{Au}_x$, respectively.

in $\text{Yb}(\text{Rh}_{1-x}\text{Ir}_x)_2\text{Si}_2$, T^* and our theoretically predicted T_{qp}^* are in the same temperature range, we conjecture that both may be of the same physical origin - the competition of fermionic CSD and quasiparticle breakdown at the QCP. As a crossover temperature, T_{qp}^* remains non-zero, but can be exceedingly small, depending on α , see inset of Fig. 3g. Note that away from criticality, we have $\alpha \rightarrow 0$ so that the logarithmic low-temperature behavior does not occur in agreement with Figs. 2e to 2g. The blue curves in Figs. 2d and 2h represent the evaluation of Eq. (1) for the spectrum $W(\hbar\omega)$ of the THz pulses used in our experiment. Considering that α is the only adjustable parameter apart from the overall signal amplitude and that we use the same value $T_K \approx 25$ K for both curves, the agreement between theory and data is excellent.

We can now extract the critical exponent α by comparing the logarithmic slope s_{low} associated with the the CSD at low temperatures ($T_{qp}^* < T < T_K$) from Eq. (2) with the slope s_{high} of the standard logarithmic behaviour of the Kondo weight at high temperature ($T > T_K$) according to $P(T) = A \ln(T_K/T)$. This directly leads to $\alpha = s_{\text{low}}/s_{\text{high}}$. From the experimental data we find $\alpha = 0.10$ for $\text{Yb}(\text{Rh}_{1-x}\text{Ir}_x)_2\text{Si}_2$ at $x = 0$, $B_{\perp} = 66$ mT in

Fig. 2d and $\alpha = 0.28$ at $x = 0.06$, $B_{\perp} = 0$ in Fig. 2h. Note that different critical behavior for QPTs by magnetic fields and chemical pressure have been observed before[28]. It is a signature of the different types of quantum-critical fluctuations in the two cases.

Our theory also explains why the logarithmic low-temperature increase of THz absorption indicating CSD cannot be observed in the $\text{CeCu}_{6-x}\text{Au}_x$ system. For this material, the ratio T_K/T^* is substantially smaller than in the $\text{Yb}(\text{Rh}_{1-x}\text{Ir}_x)_2\text{Si}_2$ system so that the effects of the buildup of Kondo weight and of the CSD overlap to such an extent that the latter is obscured, as seen in Fig. 3h and in agreement with experiment[14].

Summarizing in Fig. 4 the measured THz absorption data in a T -versus- B phase diagram reveals that on the HF liquid side of the QCP ($B_{\perp} > 66$ mT) $P(T)$ is enhanced for $T < 10$ K due to the CSD effect and as explained by our two-band HF liquid theory. By contrast, on the antiferromagnetic side ($B_{\perp} \lesssim 50$ mT) we observe a reduction of the Kondo-weight-related absorption but no fermionic CSD. This suggests that in this region the RKKY interaction strongly affects the quasiparticle dynamics such that the the two-band HF liquid theory is not valid here[19–21].

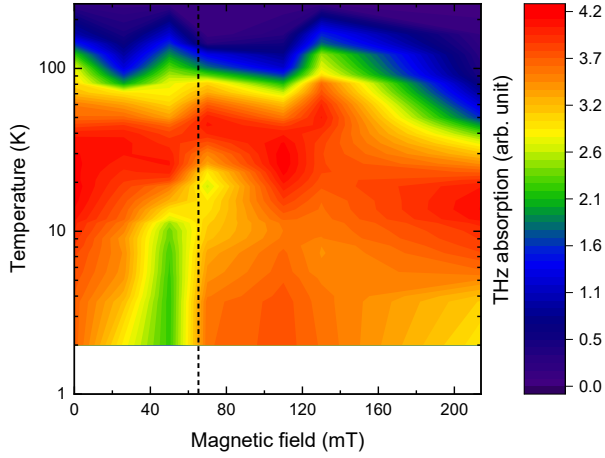


Figure 4. **Phase diagram of field-tuned YbRh_2Si_2** as measured by THz time-delay spectroscopy, using the discrete magnetic-field values shown in Fig. 2. The color code represents the resonant THz absorption, and the dashed line marks the critical field of 66 mT.

To conclude, we observed a logarithmic low-temperature increase in the resonant quasiparticle excitation probability $P(T)$ near a magnetic quantum phase transition in heavy-fermion materials. We identified this logarithmic increase as a unique signature of fermionic quasiparticle CSD, that is, a vanishing quasiparticle frequency, near a quantum phase transition with fermionic breakdown. Since, in contrast to thermodynamic and transport properties, our time-resolved THz spectroscopy is exclusively sensitive to the HF quasiparticle dynamics as opposed to thermal fluctuations, we could further extract the fermionic critical exponent α of the vanishing quasiparticle weight. The critical behaviour of α suggests to define the heavy quasiparticle weight as an order parameter for quantum phase transitions with fermionic breakdown. It also sets the stage for a classification of fermionic quantum phase transitions in terms of their critical exponent, analogous to thermodynamic phase transitions.

Methods

Experimental

Single-crystalline, c -oriented $\text{Yb}(\text{Rh}_{1-x}\text{Ir}_x)_2\text{Si}_2$ platelets ($x = 0, 0.06$) with dimensions of $2 \times 3 \times 0.07 \text{ mm}^3$ were grown from indium flux as described in the literature[23]. The sample surface is freshly polished before the THz measurements. Samples are mounted onto a Teflon holder, where two permanent magnets placed above and below the sample generate a magnetic field of up to 214 mT in the easy magnetic plane perpendicular to the tetragonal c -axis. We use a temperature-controlled Janis SVT-400 helium-reservoir cryostat operable in the range from 1.9 to 325 K. The THz experiments are performed in a 90° reflection geometry with THz light in a spectral range from 0.1 to 3 THz polarized perpendicular to the crystallographic c -axis.

We generate single-cycle THz pulses by optical rectification in a 0.5-mm-thick (110)-cut ZnTe single crystal, using 90% of an amplified Ti:Sapphire laser output (wavelength 800 nm, pulse duration 50 fs, pulse repetition rate 1 kHz, 2.5 mJ pulse energy).

The energy of the THz pulse is in the range of a few nJ. The residual 10% of the 800-nm beam is then used for free-space electro-optic sampling of the reflected THz light from the sample. Both, the THz and the 800-nm beams, are collinearly focused onto a 0.5-mm-thick (110)-cut ZnTe detection crystal. To increase the accessible time delay between the THz and the 800-nm pulses, Fabry-Pérot resonances from the faces of the detection crystal are suppressed by a 2-mm-thick THz-inactive (100)-cut ZnTe crystal. The THz-inactive crystal is optically bonded to the back of the detection crystal. The THz-induced ellipticity of the 800-nm beam is measured using a quarter-wave plate, a Wollaston prism and a balanced photodiode.

Theoretical

We construct a phenomenological, critical two-band Fermi liquid theory to describe the THz-induced resonant transitions from the heavy conduction to the light valence band. Electrons in the light band have the dispersion $\epsilon_p^{(0)}$ measured relative to the Fermi energy E_F , have spectral weight unity, and are assumed to be non-interacting. The parameters of the heavy electron states, generated by the Kondo effect, are controlled by the Kondo scale T_K . Their energy lies close to the Fermi level E_F , shifted by $\Delta \approx \pm k_B T_K$ above (particle-like HF systems) or below (hole-like HF systems) E_F [3, 26]. They have a strongly reduced spectral weight $a(T)$ which reaches $a(0) = T_K/\gamma \ll 1$ at $T = 0$ and decreases logarithmically for temperatures $T > T_K$ [3]. Here, γ is the effective hybridization of the rare-earth $4f$ orbitals with the conduction electron states. We also take a residual interaction of the quasiparticles within the heavy band into account. It implies an additional reduction of both, the quasiparticle weight and of the heavy band shift, by the local quasiparticle weight factor $z_0(T)$ (see main text), $a \rightarrow z_0 a$, $\Delta \rightarrow z_0 \Delta$. Taking now the hybridization V between the light, uncorrelated band and the heavy band into account and calculating the hybridized band structure, the band energies are obtained as

$$\epsilon_{1,2\bar{p}} = \frac{1}{2} \left[\epsilon_{\bar{p}}^{(0)} + z_0 \Delta \pm \sqrt{(\epsilon_{\bar{p}}^{(0)} - z_0 \Delta)^2 + 4z_0 a |V|^2} \right], \quad (3)$$

and are shown, for different temperatures, in Figs. 2d to 2f. Due to the hybridization, the quasiparticle weights in the lower (1) and upper (2) bands become momentum dependent and read

$$z_{1,2\bar{p}} = \frac{(1 + z_0 a)(\epsilon_{1,2\bar{p}} - z_0 \Delta) - z_0 a(\epsilon_{\bar{p}}^{(0)} - z_0 \Delta)}{2(\epsilon_{1,2\bar{p}} - z_0 \Delta) - (\epsilon_{\bar{p}}^{(0)} - z_0 \Delta)}, \quad (4)$$

as shown in Figs. 2a to 2c. Inserting these expressions into Eq. (1) and adjusting the two parameters T_K/D and α , where D is the free conduction bandwidth, leads to the curves shown in Figs. 2d, h and 3g, h. Symmetry implies that this result for the THz absorption is the same for particle-like and hole-like HF systems.

Acknowledgement.

This work was financially supported by the Swiss National Science Foundation (SNSF) via project No. 200021_178825 (M.F., S.P., C.J.Y.) and by the Deutsche Forschungsgemeinschaft (DFG) via SFB/TR 185 (277625399) OSCAR and the

Cluster of Excellence ML4Q (90534769, project C4) (J.K.) as well as via SFB/TRR 288 (422213477, project A03) and grant no. KR3831/4-1 (K.K., C.K.). S.P. further acknowledges the support by ETH Career Seed Grant SEED-17 18-1.

Author contributions.

All authors contributed to the discussion and interpretation of the experiment and to the completion of the manuscript. S.P. and C.J.Y. performed the experiment and the data analysis. K.K. and C.K. provided the YbRh_2Si_2 and $\text{Yb}(\text{Rh}_{0.94}\text{Ir}_{0.06})_2\text{Si}_2$ samples. J.K. performed the theoretical analysis. J.K. and M.F. conceived the work, and S.P. supervised the experiments. S.P., J.K. and M.F. drafted the manuscript.

Competing interests.

The authors declare that they have no competing financial interests.

Correspondence.

Correspondence and requests for materials should be addressed to, M.F. (email: manfred.fiebig@mat.ethz.ch), J.K. (email: kroha@physik.uni-bonn.de) or S.P. (email: shovon.pal@niser.ac.in)

-
- [1] Reichl, L. E. *A Modern Course in Statistical Physics*, 4th edn (Wiley-VCH, 2016).
 - [2] Kondo, J. Resistance minimum in dilute magnetic alloys. *Prog. Theor. Phys.* **32**, 37 (1964).
 - [3] Hewson, A. C. *The Kondo Problem to Heavy Fermions* (Cambridge Univ. Press, 1993).
 - [4] Si, Q., Rabello, S., Ingersent, K., & Smith, J. L. Locally critical quantum phase transitions in strongly correlated metals. *Nature* **413**, 804 (2001).
 - [5] Coleman, P., Pépin, C., & Si, Q., & Ramazashvili, R. How do Fermi liquids get heavy and die?. *J. Phys. Condens. Matter* **13**, R723 (2001).
 - [6] von Löhneysen, H., Rosch, A., Vojta, M., & Wölfle, P. Fermi-liquid instabilities at magnetic quantum phase transitions. *Rev. Mod. Phys.* **79**, 1015 (2007).
 - [7] Gegenwart, P., Westerkamp, T., Krellner, C., Tokiwa, Y., Paschen, S., Geibel, C., Steglich, F., Abrahams, E., & Si, Q. Multiple Energy Scales at a Quantum Critical Point. *Science* **315**, 969 (2007).
 - [8] Schröder, A., Aeppli, G., Coldea, R., Adams, M., Stockert, O., von Löhneysen, H., Bucher, E., Ramazashvili, R., & Coleman, P. Onset of antiferromagnetism in heavy-fermion metals. *Nature* **407**, 351 (2000).
 - [9] Custers, J., Gegenwart, P., Wilhelm, H., Neumaier, K., Tokiwa, Y., Trovarelli, O., Geibel, C., Steglich, F., Pépin, C., & Coleman, P. The break-up of heavy electrons at a quantum critical point. *Nature* **424**, 524 (2003).
 - [10] Paschen, S., Lühmann, T., Wirth, S., Gegenwart, P., Trovarelli, O., Geibel, C., Steglich, F., Coleman, P., & Si, Q. Hall-effect evolution across a heavy-fermion quantum critical point. *Nature* **432**, 881 (2004).
 - [11] Prochaska, L., Li, X., MacFarland, D. C., Andrews, A. M., Bonta, M., Bianco, E. F., Yazdi, S., Schrenk, W., Detz, H., Limbeck, A., Si, Q., Ringe, E., Strasser, G., Kono, J. & Paschen, S. Singular charge fluctuations at a magnetic quantum critical point. *Science* **367**, 285 (2020).
 - [12] Hackl, A., & Vojta, M. Kondo volume collapse, Kondo breakdown, and Fermi surface transitions in heavy-fermion metals. *Phys. Rev. B* **77**, 134439 (2008).
 - [13] Wölfle, P., & Abrahams, E. Quasiparticles beyond the Fermi liquid and heavy fermion criticality. *Phys. Rev. B* **84**, 041101(R) (2011).
 - [14] Wetli, C., Pal, S., Kroha, J., Kliemt, K., Krellner, C., Stockert, O., von Löhneysen, H., & Fiebig, M. Time-resolved collapse and revival of the Kondo state near a quantum phase transition. *Nat. Phys.* **14**, 1103 (2018).
 - [15] Pal, S., Wetli, C., Zamani, F., Stockert, O., von Löhneysen, H., Fiebig, M., & Kroha, J. Fermi Volume Evolution and Crystal-Field Excitations in Heavy-Fermion Compounds Probed by Time-Domain Terahertz Spectroscopy. *Phys. Rev. Lett.* **122**, 096401 (2019).
 - [16] Yang, C.-J., Pal, S., Zamani, F., Kliemt, K., Krellner, C., Stockert, O., von Löhneysen, H., Kroha, J., & Fiebig, M. Terahertz Conductivity of Heavy-fermion Systems from Time-resolved Spectroscopy. *Phys. Rev. Research* **2**, 033296 (2020).
 - [17] Trovarelli, O., Geibel, C., Mederle, S., Langhammer, C., Grosche, F. M., Gegenwart, P., Lang, M., Sparn, G. & Steglich, F. YbRh_2Si_2 : Pronounced Non-Fermi-Liquid Effects above a Low-Lying Magnetic Phase Transition. *Phys. Rev. Lett.* **85**, 626 (2000).
 - [18] Gegenwart, P., Custers, J., Geibel, C., Neumaier, K., Tayama, T., Tenya, K., Trovarelli, O., & Steglich, F. Magnetic-field induced quantum critical point in YbRh_2Si_2 . *Phys. Rev. Lett.* **89**, 056402 (2002).
 - [19] Ruderman, M. A. & Kittel, C. Indirect exchange coupling of nuclear magnetic moments by conduction electrons. *Phys. Rev.* **96**, 99 (1954).
 - [20] Kasuya, T. A Theory of Metallic Ferro- and Antiferromagnetism on Zener's Model. *Prog. Theor. Phys.* **16**, 45 (1956).
 - [21] Yosida, K. Magnetic properties of Cu-Mn alloys. *Phys. Rev.* **106**, 893 (1957).
 - [22] Nejati, A., Ballmann, K., & Kroha, J. Kondo Destruction in RKKY-Coupled Kondo Lattice and Multi-Impurity Systems. *Phys. Rev. Lett.* **118**, 117204 (2017).
 - [23] Krellner, C., Taube, S., Westerkamp, T., Hossain, Z., & Geibel, C. Single-crystal growth of YbRh_2Si_2 and YbIr_2Si_2 . *Philos. Mag.* **92**, 2508 (2012).
 - [24] Friedemann, S., Westerkamp, T., Brando, M., Oeschler, N., Wirth, S., Gegenwart, P., Krellner, C., Geibel, C., & Steglich, F. Detaching the antiferromagnetic quantum critical point from the Fermi-surface reconstruction in YbRh_2Si_2 . *Nat. Phys.* **5**, 465 (2009).
 - [25] Paschen, S., Friedemann, S., Wirth, S., Steglich, F., Kirchner, S., & Si, Q. Kondo destruction in heavy fermion quantum criticality and the photoemission spectrum of YbRh_2Si_2 . *Magn. Magn. Mater.* **400**, 17 (2016).
 - [26] Q. Y., Xu, D. F., Niu, X. H., Jiang, J., Peng, R., Xu, H. C., Wen, C. H. P., Ding, Z. F., Huang, K., Shu, L., Zhang, Y. J., Lee, H., Strocov, V. N., Shi, M., Bisti, F., Schmitt, T., Huang, Y. B., Dudin, P., Lai, X. C., Kirchner, S., Yuan, H. Q., & Feng, D. L. Direct observation of how the heavy-fermion state develops in CeCoIn_5 . *Phys. Rev. B* **96**, 045107 (2017).
 - [27] P. Gegenwart, P., Tokiwa, Y., Westerkamp, T., Weickert, F., Custers, J., Ferstl, J., Krellner, C., Geibel, C., Kersch, P., Müller, K.H. & Steglich, F. High-field phase diagram of the heavy-fermion metal YbRh_2Si_2 . *New J. Phys.* **8**, 171 (2006).
 - [28] von Löhneysen, H., Pfeleiderer, C., Pietrus, T., Stockert, O. & Will, B. Pressure versus magnetic-field tuning of a magnetic quantum phase transition. *Phys. Rev. B* **63**, 134411 (2001).